

1. Introduction

The American Cancer Society estimates that more than 1.7 million people will be diagnosed with cancer and more than 600,000 of them will die in 2018. (Siegel 2018). Surgery to remove tumors is the primary method of treatment for solid mass tumors. The objective of the surgery is to remove all diseased tissue while minimizing damage to adjacent healthy tissue to preserve function and/or for cosmetic reasons. A significant challenge for cancer surgery is ensuring that no residual malignant tissue is left behind as recurrent tumors lead to high mortality rates. Consequently, the success of cancer surgery depends on a doctor's ability to accurately delineate tumor margins. Paraffin section of inked surgical margins is the gold standard for margin assessment. Unfortunately, this process is time consuming and results are not available until several days after surgery. Typically, surgeons determine the tumor resection margins during procedures based on palpation, visual inspection and frozen section histology. Cancer surgeons need additional intraoperative imaging modalities for use during surgery to clearly delineate tumor margins and identify areas of residual disease. To address this problem, the Biomedical Imaging Lab at UNC Charlotte has constructed a single-pixel hyperspectral imaging (HSI) system to examine the optical spectra of tissue to detect cancer margins (Peller 2018).

Recent research has demonstrated that optical spectroscopy can be used to distinguish between healthy and diseased tissue (e.g. Volynskaya 2008; Zonios 1999; Georgakoudi 2001). Cancer detection via optical spectroscopy is based on the biochemical and morphological changes that occur in malignant tissue. Both reflectance and autofluorescence spectroscopy have been shown to effectively identify diseased tissue. Autofluorescence emission is produced by the natural constituents of tissue when the tissue is illuminated by a UV source. The autofluorescence of collagen, near 400 nm, and nicotinamide adenine dinucleotide phosphate, NAD(P)H, near 475 nm, have been noted for their high sensitivity to the presence of a range of different cancers (Ramanujam 1994; Schomacker 1992; Cothren 1990). Reflectance spectroscopy provides information about tissue cell size and density. To obtain a reflectance spectrum, a white light source illuminates an object and the reflected light is captured by a spectrometer. Alterations in tissue morphology, including hyperplasia, nuclear crowding, and increased nuclear/cytoplasmic ratio are associated with disease progression and can cause changes in the wavelength dependence of the reflected spectrum (e.g. Lu 2014).

The research project described here supports the development of the new HSI imaging system for cancer detection. A well-defined tissue model is needed to validate the ability of the HSI system to detect changes in tissue properties via optical spectroscopy. In this study, we detect changes in autofluorescence and reflectance spectra in porcine skin *ex vivo*. The study investigates the changes in the spectra of tissue caused by thermal and chemical damage and which type of spectroscopy (reflectance or fluorescence) most accurately detects that damage.

2. Methods

Porcine skin of uniform thickness (1 cm) was cut into approximately 5 cm squares. Reflectance and fluorescence spectra of the healthy tissue samples were obtained. The tissue was then damaged using one of three methods (thermal contact, laser, or chemical) and the reflectance and fluorescence spectra of the damaged samples were collected. An Ocean Optics QE-Pro spectrometer with a fiber optic cable was used to obtain the spectra. A 300W Xenon light source was used to illuminate the tissue sample for reflectance. A nitrogen laser (335 nm; SRS, NL100) was used to excite the fluorescent emission in the samples. Oceanview software was used to analyze the data. A schematic of the experimental setup is shown in Figure 1.

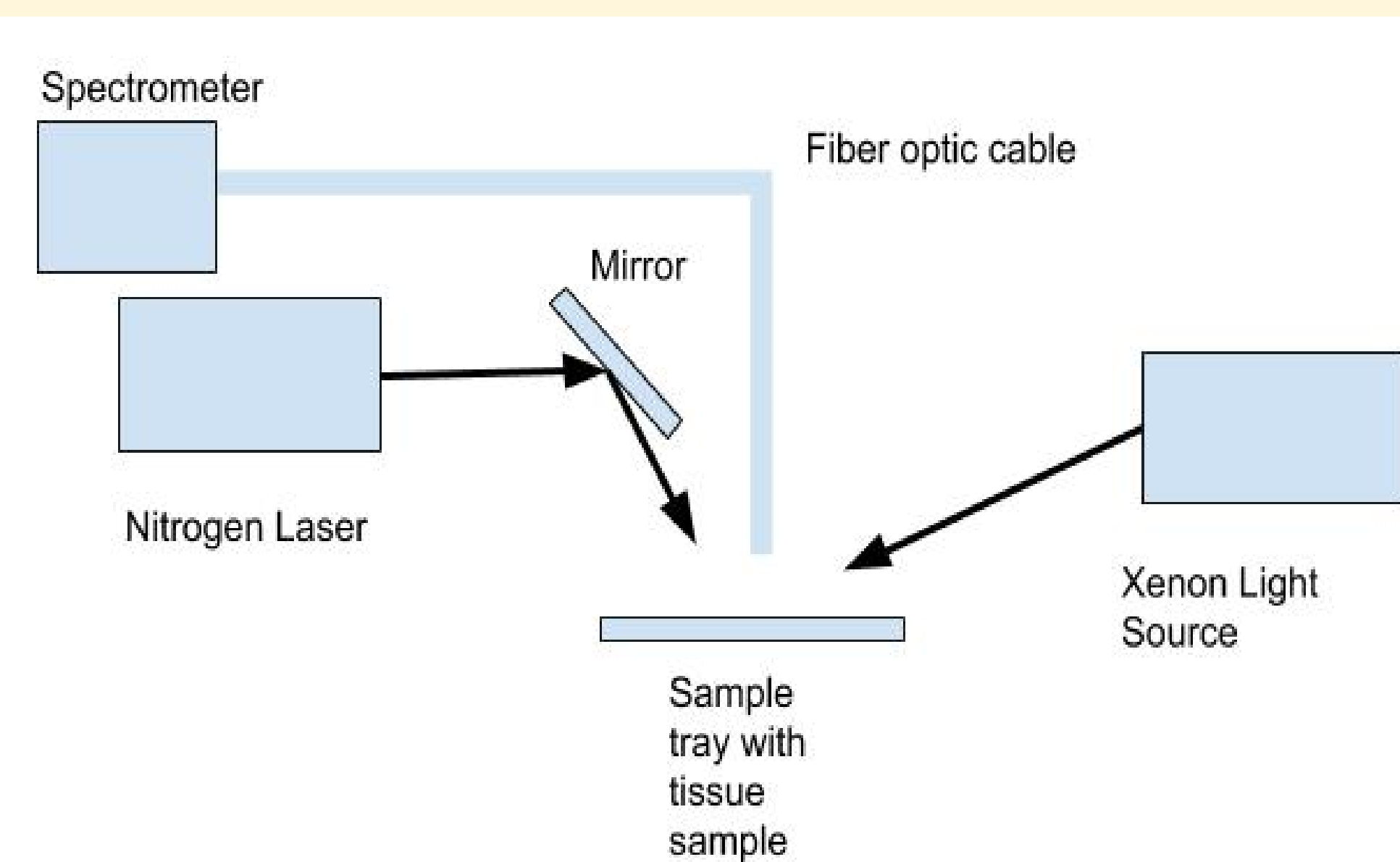


Figure 1. Experimental setup for reflectance and fluorescence spectroscopy.

Six samples were chemically damaged using 0.36M HCl applied to the surface of the tissue. The acid remained on the tissue for approximately 10 minutes and the samples were then rinsed with deionized water. The size of the damaged area on each tissue sample was approximately 1.5 cm.

3. Results and Analysis

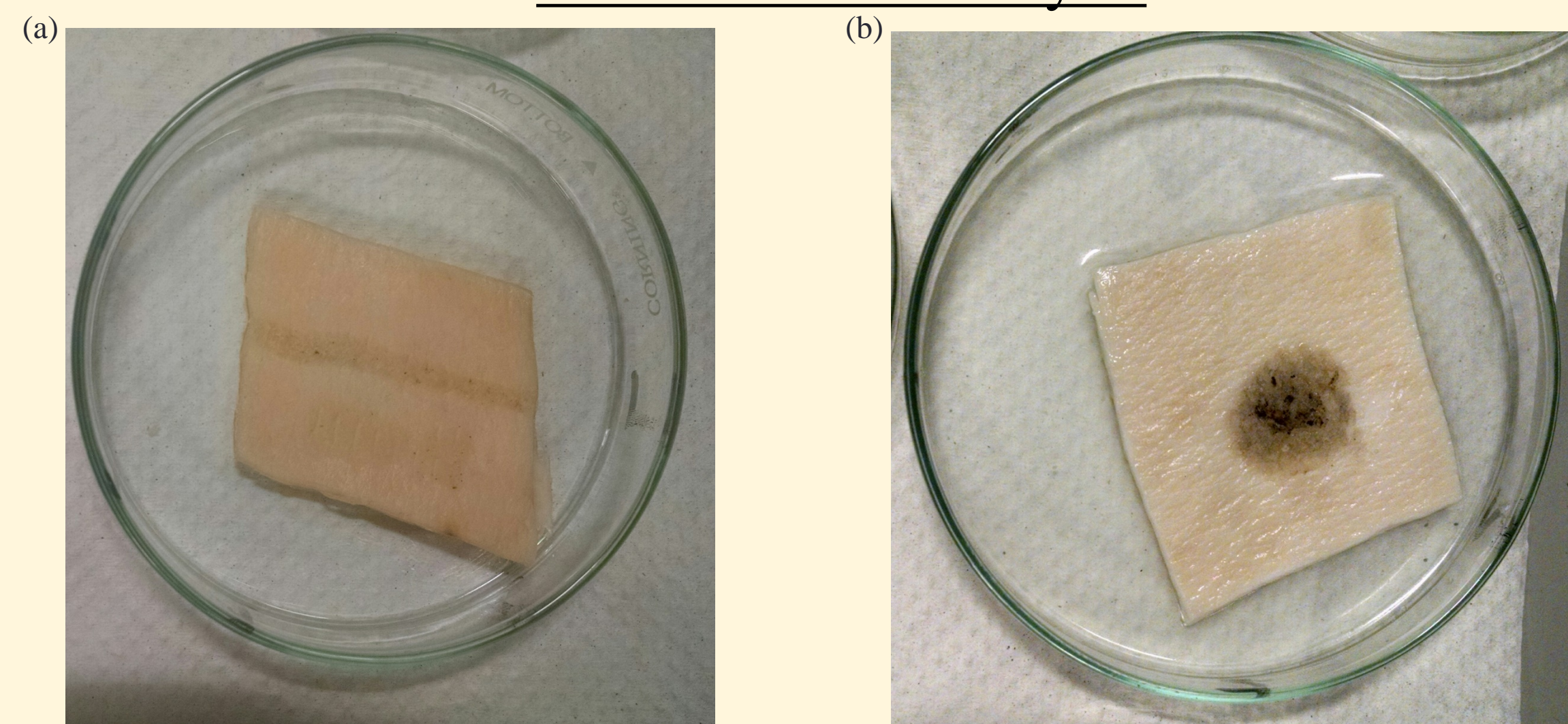


Figure 2. (a) Straight line damage from thermal contact on porcine skin tissue sample 1. (b) Circular damage from thermal contact on porcine skin tissue sample 2.

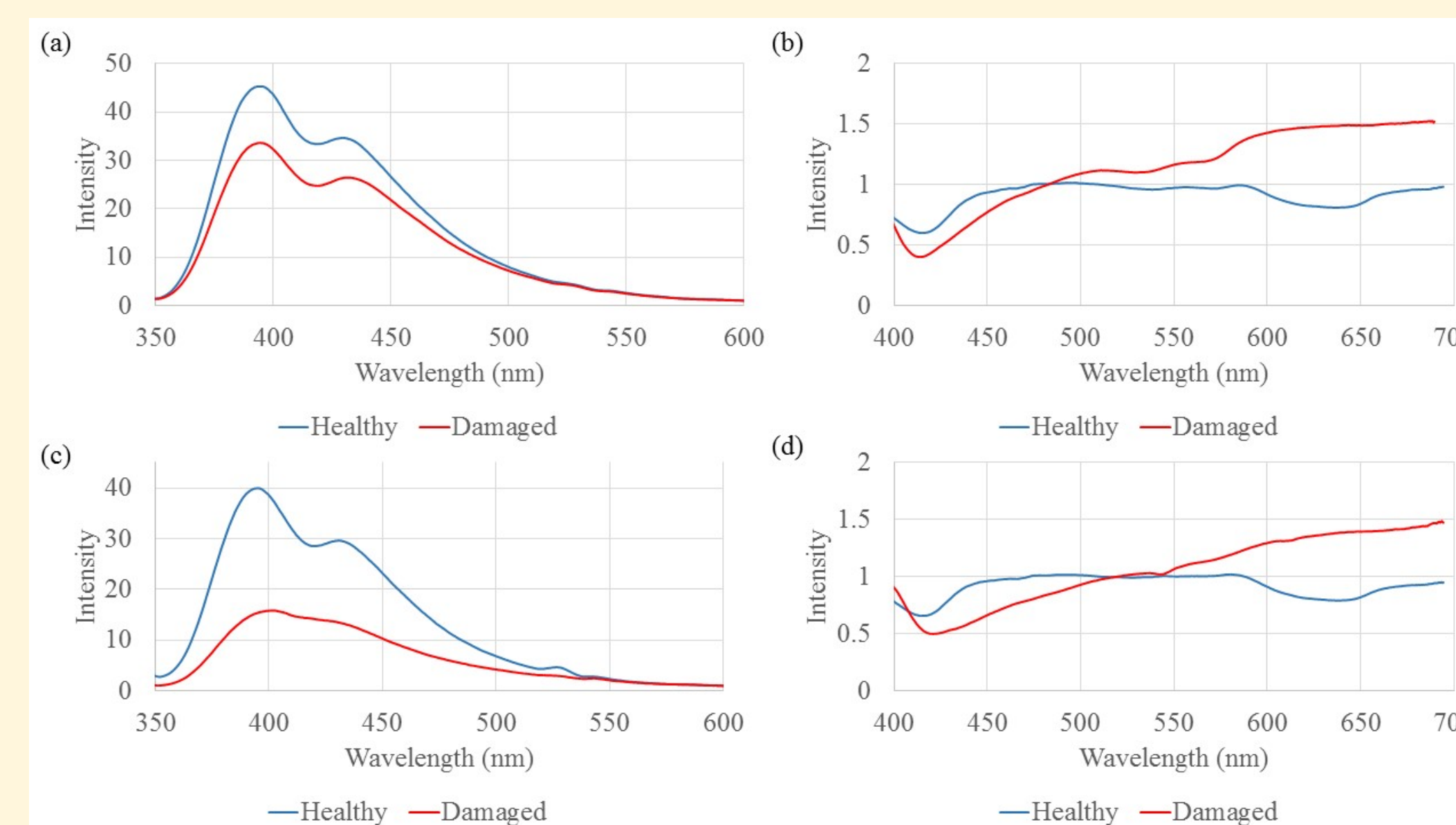


Figure 3. Normalized (a) autofluorescence and (b) reflectance spectra of healthy tissue and tissue thermally damaged via contact for tissue Sample 1. Normalized (c) autofluorescence and (d) reflectance spectra of healthy tissue and tissue thermally damaged via contact for tissue Sample 2.

3.1 Thermal Contact Damage

In Sample 1, the tissue was thermally damaged via contact with a hot object in a straight line across the center of the sample (See Fig. 2a). In Sample 2, a large circular area was damaged and included some visible charring of the tissue (See Fig. 2b). The spectra of Samples 1 and 2 are shown in Figure 3. Both the autofluorescent and reflectance spectra change after thermal damage. In the autofluorescent spectrum, the peak near 400 nm is emission from collagen and the peak near 440 nm is NAD(P)H. The thermal damage alters/destroys the structure of the collagen and NAD(P)H proteins, resulting in a decrease in the fluorescent emission of these molecules. The change in the fluorescent spectrum for Sample 2 is more pronounced. This is likely due to more significant thermal damage in this sample as indicated by the presence of charring. The reflectance spectra of Samples 1 and 2 are also displayed in Figure 3. A noticeable difference between healthy and damaged tissues is evident. This indicates that the morphology and/or color of the tissue has been changed. For both the autofluorescent and reflectance spectra, changes in the optical properties of the tissue as a result of thermal contact damage are evident. This type of damage can provide a good tissue model to test the HSI system.

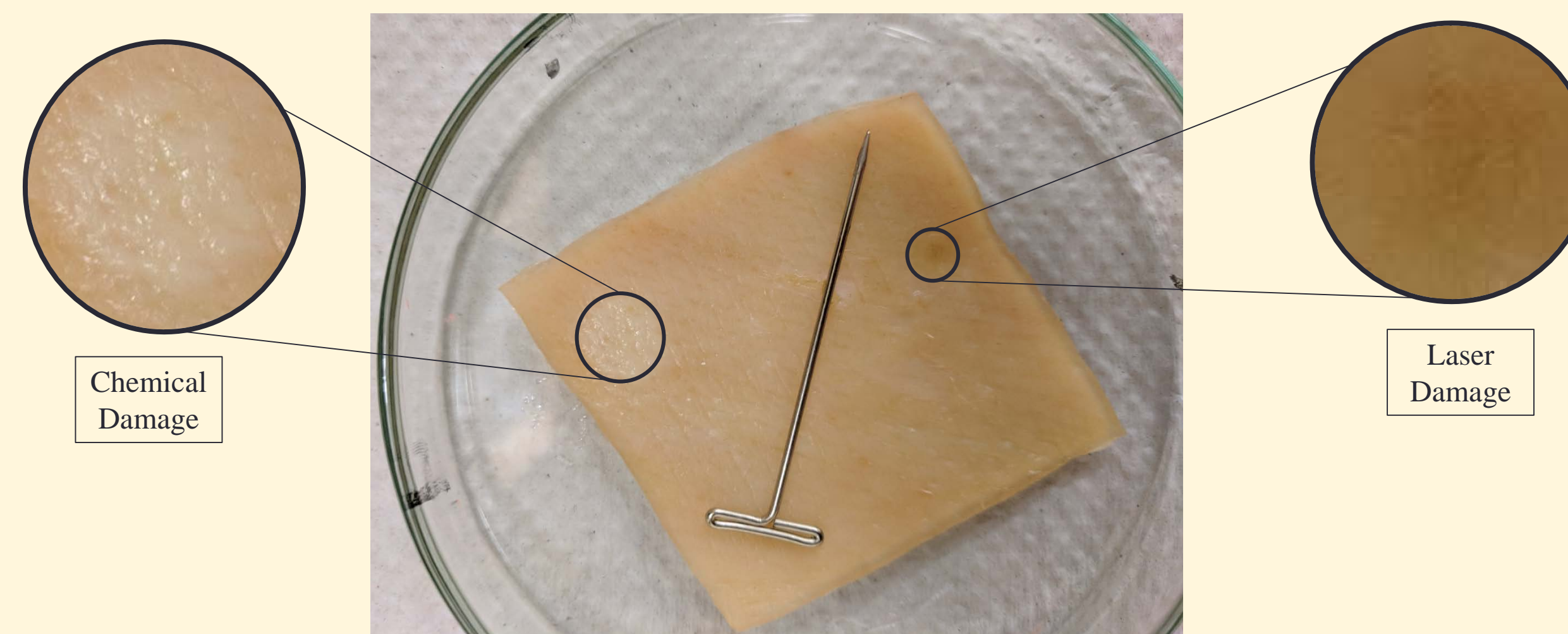


Figure 4. Skin tissue sample with chemical and laser damage.

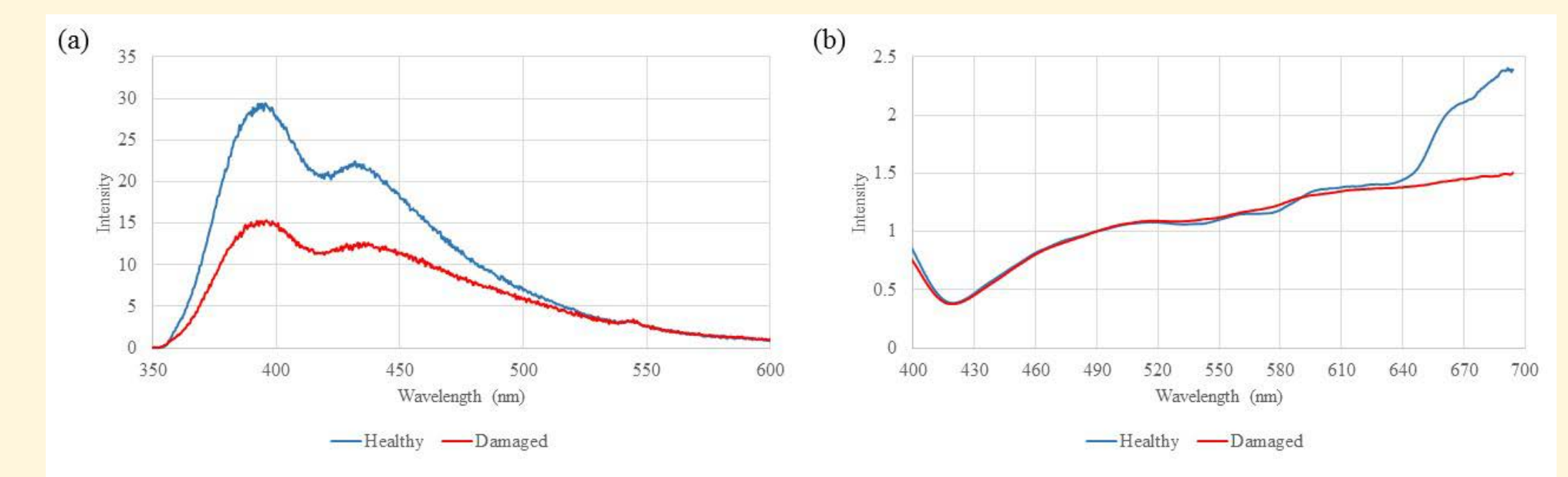


Figure 5. Normalized (a) fluorescence and (b) reflectance graphs of healthy and laser damaged areas of a non-hydrated porcine tissue sample.

3.2 Laser Damage

Irradiation with the 1064 nm laser resulted in a circular region of damage on the tissue (see Figure 4). Figure 5 shows the autofluorescence and reflectance spectra of a representative tissue sample. When the tissue samples were damaged with the laser, the collagen and NAD(P)H emission peaks were suppressed, indicating that these proteins were damaged/destroyed by laser irradiation. The reflectance spectra, however, only show a noticeable change at long wavelengths (> 640 nm). For the autofluorescent spectra, changes in the optical properties of the tissue as a result of laser damage are evident. However, the changes in the reflectance spectra are more subtle. Laser damage can provide a good tissue model to test the HSI system in fluorescence mode, but may not be ideal for reflectance.

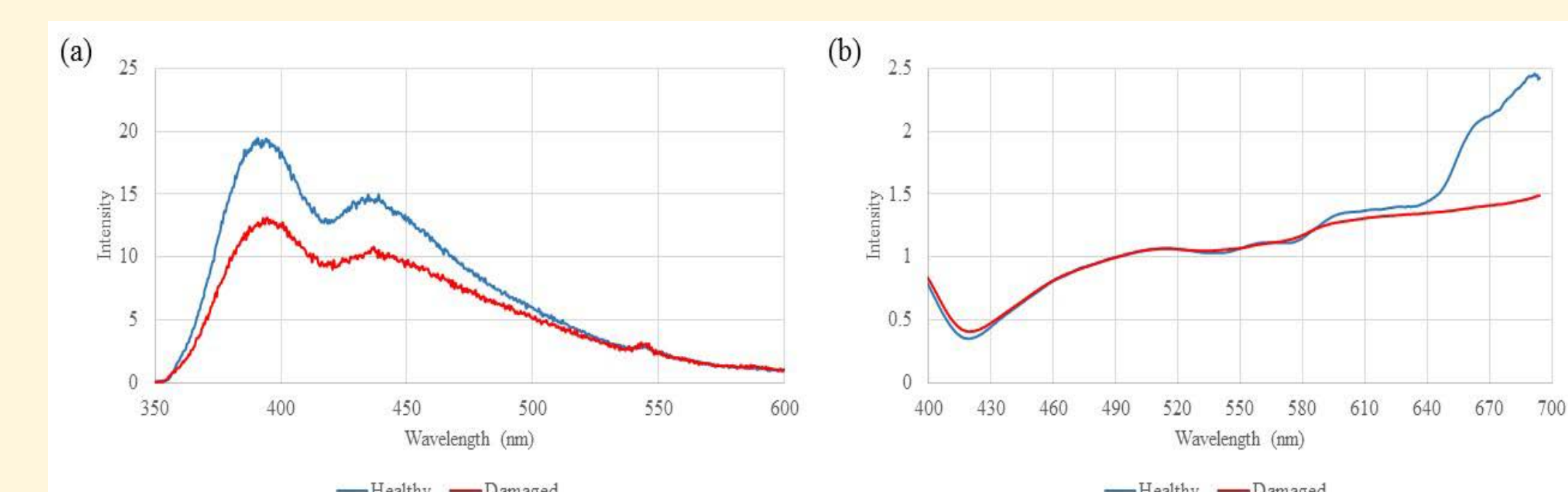


Figure 6. Normalized (a) fluorescence and (b) reflectance graphs of healthy and chemically damaged areas of a non-hydrated porcine tissue sample.

3.3 Chemical Damage

Figure 4 shows the region of chemical damage on a sample of porcine skin tissue. Figure 6 shows the autofluorescence and reflectance spectra of the skin samples before and after the damage with 0.36 M HCl. The emission peaks of the collagen and NAD(P)H are weaker after chemical damage, however the reflectance spectra changes only at longer wavelengths (> 640 nm). These alterations in the spectra are similar to those seen for the laser damage. For the autofluorescent spectra, changes in the optical properties of the tissue as a result of chemical damage are evident. However, the changes in the reflectance spectra are more subtle. Chemical damage can provide a good tissue model to test the HSI system in fluorescence mode, but may not be ideal for reflectance.

4. Conclusions and Future Work

- Thermal contact damage resulted in significant changes to both the autofluorescence and reflectance spectra of the tissue. This damage method resulted in the largest change in the reflectance spectra. Thermal contact damage seems to be the best to use for future models of unhealthy tissue.
- The laser and chemical damage altered the fluorescence spectra significantly, but had little effect on the reflectance spectra.
- Using a larger diameter/longer wavelength laser to damage the tissue might show more change in the reflectance/fluorescence spectra.
- These tissue models will be used to validate the ability of the HSI system to detect unhealthy tissue in future studies.

Acknowledgements

This research was supported by Charlotte Teachers Institute, the Department of Physics and Optical Science at UNC Charlotte, and Charlotte Community Scholars.

References

- Cothren, R. M., Richards-Kortum, R., Sivak, M. V., Fitzmaurice, M., Rava, R. P., Boyce, G. A., ... & Feld, M. S. (1990). Gastrointestinal tissue diagnosis by laser-induced fluorescence spectroscopy at endoscopy. *Gastrointestinal Endoscopy*, 36(2), 105-111.
- Georgakoudi, I., Jacobson, B. C., Van Dam, J., Backman, V., Wallace, M. B., Müller, M. G., ... & Perelman, L. T. (2001). Fluorescence, reflectance, and light-scattering spectroscopy for evaluating dysplasia in patients with Barrett's esophagus. *Gastroenterology*, 120(7), 1620-1629.
- Lu, G., & Fei, B. (2014). Medical hyperspectral imaging: a review. *Journal of biomedical optics*, 19(1), 010901-010901.
- Peller, J., Farahi, F., & Trammell, S. R. (2018). A hyperspectral imaging system based on a single-pixel camera design for detecting differences in tissue properties. *Applied Optics*, accepted.
- Ramanujam, N., Mitchell, M. F., Mahadevan, A., Warren, S., Thomsen, S., Silva, E., & Richards-Kortum, R. (1994). In vivo diagnosis of cervical intraepithelial neoplasia using 337-nm-excited laser-induced fluorescence. *Proceedings of the National Academy of Sciences*, 91(21), 10193-10197.
- Schomacker, K. T., Frisoli, J. K., Compton, C. C., Flotte, T. J., Richter, J. M., Nishioka, N. S., & Deutsch, T. F. (1992). Ultraviolet laser-induced fluorescence of colonic tissue: basic biology and diagnostic potential. *Lasers in surgery and medicine*, 12(1), 63-78.
- Siegel, R. L., Miller, K. D., and Jemal, A. (2018). Cancer statistics, 2018. *CA: A Cancer Journal for Clinicians*, 68(1), 7-30. doi:10.3322/caac.21442
- Volynskaya, Z., Haka, A. S., Bechtel, K. L., Fitzmaurice, M., Shenk, R., Wang, N., ... & Feld, M. S. (2008). Diagnosing breast cancer using diffuse reflectance spectroscopy and intrinsic fluorescence spectroscopy. *Journal of biomedical optics*, 13(2), 024012-024012.
- Zonios, G., Perelman, L. T., Backman, V., Manoharan, R., Fitzmaurice, M., Van Dam, J., & Feld, M. S. (1999). Diffuse reflectance spectroscopy of human adenomatous colon polyps in vivo. *Applied Optics*, 38(31), 6628-6637.